



Enhancement of Semiconductor Properties of ZnO and Cu₂O for Photovoltaic Applications

¹*Malka Kariyawasm, ²Jinasena Hewage

¹Department of Chemistry, University of Ruhuna, Sri Lanka

²Department of Natural Sciences, Dickinson State University, ND 58601, USA

Email of the Corresponding Author - *malka.kariyawasam@gmail.com

ARTICLE INFO

Article History:

Received: 10 September 2023

Accepted: 01 November 2023

Keywords:

Photovoltaics; ZnO NPs; Cu₂O NPs; Co co-doped Ag-ZnO NPs; Solar cell

Citation:

Malka Kariyawasm and Jinasena Hewage. (2023). Enhancement of Semiconductor Properties of ZnO and Cu₂O for Photovoltaic Applications. Proceedings of SLIIT International Conference on Advancements in Sciences and Humanities, 1-2 December, Colombo, pages 346-352.

ABSTRACT

The Photovoltaics phenomenon is one of the major turning points in the battle against the depletion of fossil fuels. Sunlight being the main resource in photovoltaics, there still remains a quest to harvest it efficiently, to generate electricity. This study is focused on designing a basic, cost-effective prototype solar cell using ZnO and Cu₂O nanoparticles (NPs) under normal university laboratory conditions. An ITO-coated glass was used as the substrate of the solar cell and a modified low-temperature chemical bath deposition method was used to fabricate the solar cell. Both ZnO and Cu₂O were synthesized by aqueous precipitation methods while cobalt co-doped Ag-ZnO NPs were synthesized by solvothermal method. The UV-spectroscopic analysis confirmed the characteristic band of ZnO-NPs at 367.5 nm, Cu₂O at 360 nm and cobalt co-doped Ag-ZnO at 378 nm. The FTIR spectrum showed sharp peaks at 460 cm⁻¹ and 606 cm⁻¹ for the corresponding Zn-O bond and Cu-O bond respectively with a broad peak at 1329 cm⁻¹ for Cu₂O FTIR, due to the chemisorbed and/or physisorbed H₂O and CO₂ molecules on the surface of nanostructure. The EDX analysis showed the presence of carbon impurity in ZnO-NPs which resulted in a deviated XRD pattern for ZnO while Cu₂O showed the characteristic XRD pattern. The solar cell, which was illuminated under three

different lux conditions had a characteristic J-V plot when measured through Gamry Potentiostat. This simple, cost-effective technique can be adopted by large-scale solar cell manufacturing firms to build small prototype solar cells.

1. INTRODUCTION

For many decades inorganic materials such as silicon dominated as the main material in building conventional solar cells.¹ Although it is true that the efficiency of such conventional solar cells is high, those solar cells require very expensive materials and energy-intensive processing techniques.¹ To overcome those limitations, solution-processed solar cells based on inorganic semiconductors which include nanostructured solar cells have emerged.¹ The main advantages of inorganic semiconductor nanoparticles are, they offer the advantage of having high absorption coefficients and size tunability.¹ By varying the size of the nanoparticles, the bandgap can be tuned therefore the absorption range can be tailored.¹ Furthermore, compared with organic nanoparticles, inorganic nanoparticles are non-toxic, hydrophilic, biocompatible and highly stable.² The main two types of semiconductor NPs used are ZnO & Cu₂O nanoparticles because ZnO/Cu₂O materials are highly abundant, cheaper, and non-toxic to humans.³ Furthermore, ZnO/Cu₂O are natural n-type and p-type semiconductors respectively.³

As mentioned above these solar cell designing methods require sophisticated fabrication techniques such as spray pyrolysis and Reactive ion etching (RIE). Thus, this project works on developing advanced materials under several parallel research projects by especially focusing on the following objectives: preparation of ZnO, cobalt co-doped Ag-ZnO, and Cu₂O nanoparticles, developing a simple fabrication technique to fabricate ZnO and Cu₂O nanoparticles on a conductive glass under normal laboratory conditions at the university and checking the

functionality of the fabricated solar cell from a current density vs. potential plot (J-V plot) under dark and illuminated conditions.

2. MATERIALS AND METHODS

Zn(CH₃COO)₂·2H₂O (zinc acetate dihydrate) and AgNO₃ (silver nitrate) were obtained from BDH company. NaOH (sodium hydroxide), Cu(NO₃)₂·3H₂O (copper(II) nitrate trihydrate), and Co(NO₃)₂·6H₂O (cobalt(II) nitrate hexahydrate) were obtained from Merck Specialities Pvt. Ltd. C₂H₂O₄·2H₂O (oxalic acid dihydrate) was obtained from Himedia Laboratories Pvt. Ltd. PEG 400 (polyethylene glycol 400) was obtained from Alpha Chemika company. d-(+)-glucose anhydrous was obtained from Fluka Chemika company. All chemicals were supplied in GPR grade and were used as received without further purification.

2.1. PREPARATION OF ZNO, CU₂O AND CO CO-DOPED AG-ZNO NPS

The present work adopted the procedure followed by Halanayake et al⁴ for ZnO NPs preparation and Amini M. et al⁵ for Cu₂O NPs preparation. The procedure presented by B. Subash et al⁶ was modified to prepare Co/Ag/ZnO-NPs.

2.2. FABRICATION AND ILLUMINATION OF SOLAR CELL

Both ZnO and Cu₂O nanoparticles were fabricated on the conductive glass substrate, by using a modified, low-temperature chemical bath deposition method. Commercially available indium tin oxide (ITO) glass was used as the substrate. The substrate was first rinsed in acetone followed by ethanol and finally with deionized water. After that, around 1 cm × 1 cm area from one end of the glass substrate was taped using masking tape to a thickness of around 1 mm on a Petri dish. Then, the prepared ZnO-NPs were deposited on the conductive side of the glass substrate up

to 1 mm thickness avoiding the taped area. The deposition of ZnO-NPs on the glass substrate was done as follows. First, the ZnO-NPs were heated to boiling in a 100 mL beaker, by a Bunsen burner, with a minimal amount of distilled water to make a paste. Then the paste was poured onto the glass substrate up to the width of the masking tape and using a micro spatula it was spread evenly. After that, the petri dish containing the glass substrate and ZnO-NPs were kept on a hot plate at 60 °C temperature for 15 minutes. During the ZnO-NP solidification process, the thickness of the masking tape was increased with, around 0.5 mm. Soon after the ZnO layer solidifies, the Cu₂O-NPs paste was prepared and fabricated following the same procedure for ZnO-NPs fabrication. After that, the glass substrate containing both ZnO and Cu₂O was kept at 60 °C for 15 minutes for the solidification of the Cu₂O layer. The temperature and the time should always control carefully, else the ZnO-NPs layer and Cu₂O-NPs layer will get cracked and the Cu₂O-NPs layer might leak into the conductive glass layer. The leaking and cracking of layers will result in the dysfunction of the solar cell. Finally, the solar cell was illuminated by one zero technology, SL-838 dimmable table lamp under three lux conditions.

3. RESULTS AND DISCUSSION

Characterization of bare ZnO and cobalt co-doped Ag-ZnO-NPs

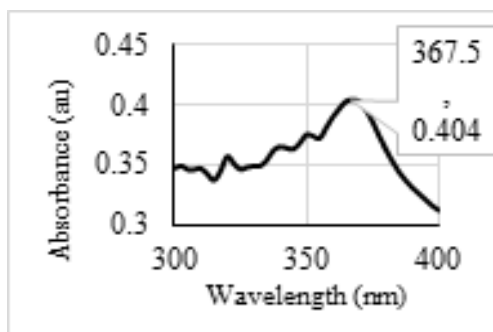


Figure 1

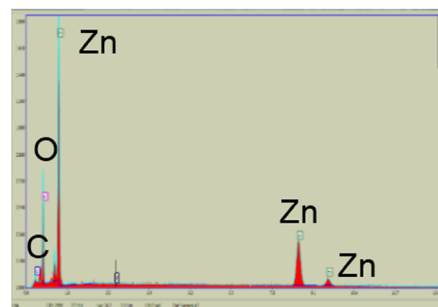


Figure 2

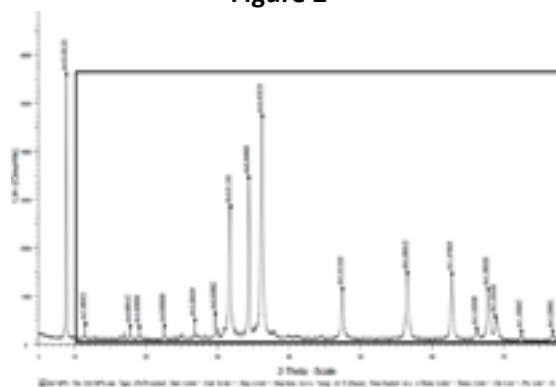


Figure 3

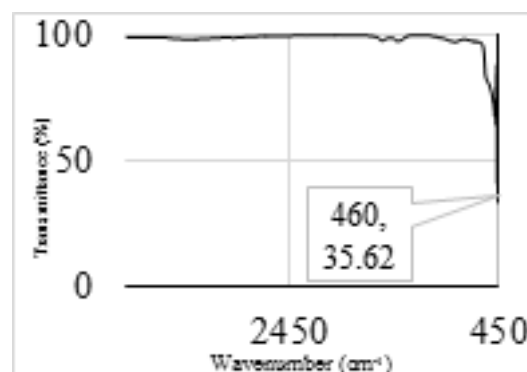


Figure 4

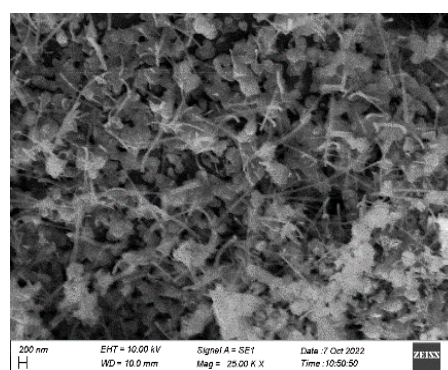


Figure 5

3.1 CHARACTERIZATION OF BARE Cu_2O -NPS AND J-V PLOT FOR $\text{ZnO}/\text{Cu}_2\text{O}$ SOLAR CELL

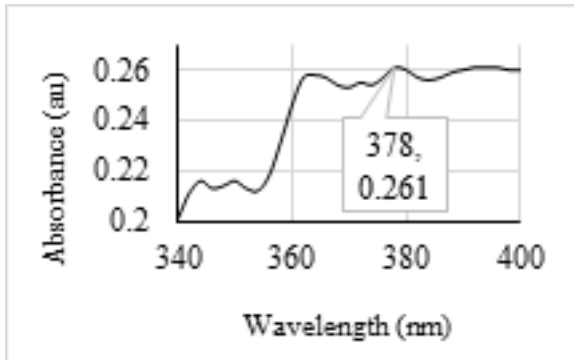


Figure 6

A wavelength scan was carried out on the range 300-400 nm for bare ZnO-NPs and Co co-doped Ag-ZnO NPs using the UH5300 Hitachi spectrophotometer. The literature UV data for ZnO-NPs is reported at 364 nm and 374 nm at pH 12.^{4,7} As shown in Figure 1 the value obtained from this study, which is 367.5 nm, is in the range between 364 nm and 374 nm, the prepared ZnO can be taken as NPs. The EDX spectrum of bare ZnO-NPs shown in Figure 2 shows that prepared NPs contain a small impurity of carbon. The XRD of the present study of bare ZnO-NPs which is shown in Figure 3 from 10-80 2(theta)-angle range (covered by the rectangular area) agrees with the literature XRD patterns.^{4,7} The 'd' values 2.81164 Å, 2.60825 Å, 2.47679 Å, 1.91304 Å, 1.62615 Å, 1.47823 Å, 1.40908 Å, 1.38005 Å, and 1.36184 Å of the graph correspond to XRD miller indices (100), (002), (101), (102), (110), (103), (200), (112), (201) respectively, which are also reported in the literature.^{4,7} The major peak between 5-10 2(theta)-angle can be accounted for carbon impurity. The FTIR data shown in Figure 4 is in close agreement with the literature values.^{7,8} The deviation from the literature range can be concluded as the presence of carbon impurities. The SEM image shown in the 200 nm range in Figure 5 confirms the formation of bare ZnO NPs. As shown in Figure 6, the current study shows a 378 nm peak for the Co co-doped Ag-ZnO NPs. The shifting of λ_{max} from 367.5 nm to 378 nm proves that the doping has worked. Thus, the band gap has been reduced paving the way to increased photovoltaic efficiencies.

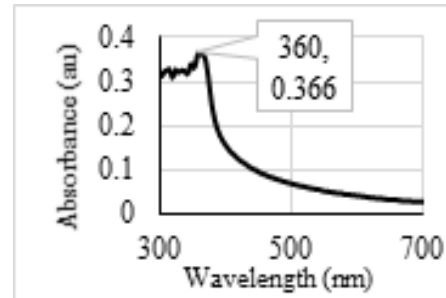


Figure 7

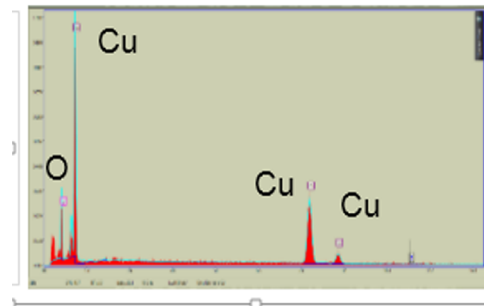


Figure 8

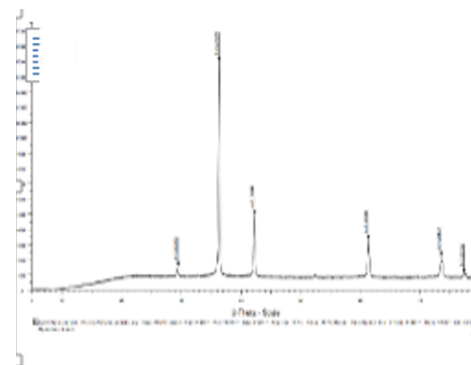


Figure 9

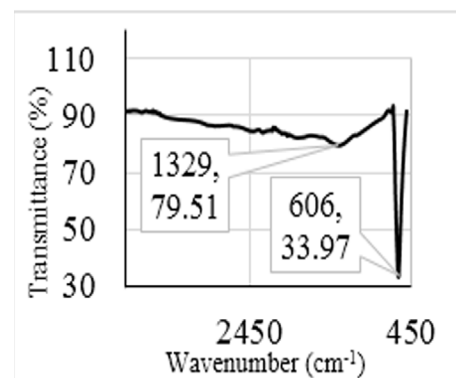


Figure 10

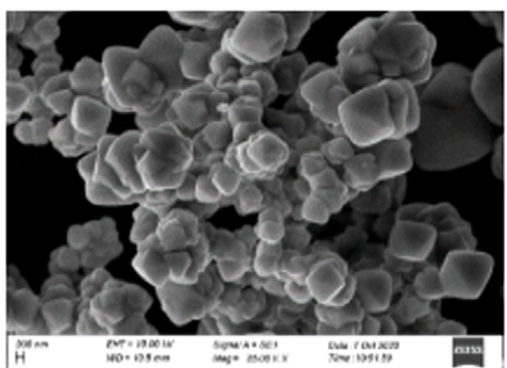


Figure 11

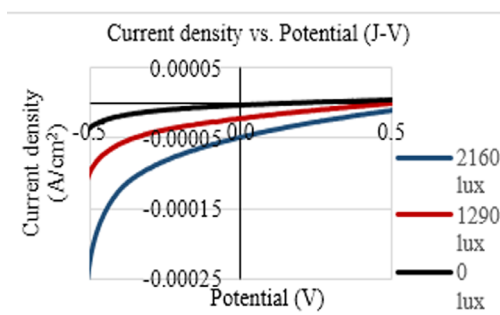


Figure 12

As shown in Figure 7, a wavelength scan was carried out on the range 300-750 nm for bare Cu₂O-NPs using UH5300 Hitachi spectrophotometer. The value obtained from the current study which is 360 nm is in good agreement with the literature values.⁹ The increase in intensity at 360 nm indicates the presence of bare Cu₂O-NPs while a decrease in intensity at 360 nm indicates the presence of CuO-NPs.^{9,10} The EDX spectrum of bare Cu₂O-NPs shown in Figure 8 shows that there are only Cu and O in the sample proving that the prepared bare Cu₂O-NPs are pure. The XRD spectra of bare Cu₂O-NPs of the current study which is shown in Figure 9, corresponds with the literature XRD patterns.⁵ The 'd' values 3.03258 Å, 2.47278 Å, 2.13686 Å, 1.50984 Å, 1.28631 Å, and 1.23194 Å of the graph correspond to XRD miller indices (110), (111), (200), (220), (311), (222) respectively, which are also reported in literature.⁵ The literature states typical Cu-O stretching of bare Cu₂O-NPs, in the range 601-624 cm⁻¹.^{10,11} Hence, the FTIR data shown in Figure 10 for prepared

bare Cu₂O-NPs are in good agreement with the literature value range. The broad absorption band between 1300 and 2000 cm⁻¹ is mainly assigned to the chemisorbed and/or physisorbed H₂O and CO₂ molecules on the surface of the nanostructure.¹² The SEM images of bare Cu₂O-NPs shown in the 200 nm range in Figure 11 confirm the formation of NPs and they are in good agreement with the literature images.⁵ The particle size analysis on both ZnO and Cu₂O NPs could not be performed at this stage due to lack of facilities and fundings. The current density vs potential plot (J-V plot) of the present study which is shown in Figure 12 follows the typical J-V curve for solar cells.^{12,13} This concludes that the designed ZnO/Cu₂O solar cell is functioning.

4. CONCLUSION

The ZnO, Co co-doped Ag-ZnO and Cu₂O NPs were successfully prepared and characterized. The λ_{max} 378 nm of Co co-doped Ag-ZnO confirms the reduction of the band gap of doped ZnO which leads the path to increased photovoltaics efficiencies of ZnO. The solar cell fabricated with ZnO/Cu₂O demonstrated the typical J-V plot, which ultimately confirms the successfulness of the prepared solar cell. Additionally, an attempt to prepare a more efficient solar cell fabricated with Co co-doped Ag-ZnO and Cu₂O was made. Since the Co-co-doped Ag-ZnO NPs appeared like a very fine powder due to calcining at 500 °C, the Co-co-doped Ag-ZnO layer was not thick enough to hold and as a result the fabrication was failed. In future work, a method can be developed to hold together Co-co-doped Ag-ZnO NPs firmly to the substrate. A study involves a concept called nanopillars to strengthen nanoparticle layers which can be inculcated in future studies.¹³

ACKNOWLEDGMENT

My appreciation goes to the Department of Chemistry, University of Ruhuna for providing me with the necessary facilities to complete my research.

REFERENCES

- Günes, S. & Sariciftci, N. S. (2008) Hybrid Solar Cells. *Inorganica Chimica Acta*, 361 (3), 581–588. <https://doi.org/10.1016/j.ica.2007.06.042>.
- Paul, W., & Sharma, C. P. (2010). Inorganic nanoparticles for targeted drug delivery. *Bio integration of Medical Implant Materials*, 204–235. <https://doi.org/10.1533/9781845699802.2.204>
- Denet, C. (2021). *Análisis y diseño de un dispositivo optoelectrónico basado en capas finas de CuO/ZnO obtenido porelectrodeposición*. *Riunet.upv.es*. <https://riunet.upv.es/handle/10251/163254#>
- Halanayake, K. D., Kalutharage, N. K., & Hewage, J. W. (2021). Microencapsulation of biosynthesized zinc oxide nanoparticles (ZnO-NPs) using Plumeria leaf extract and kinetic studies in the release of ZnO-NPs from microcapsules. *SN Applied Sciences*, 3(1). <https://doi.org/10.1007/s42452-020-04100-0>
- Amini, M., Ramezani, S., Anbari, A. P., Beheshti, A., Gautam, S., & Chae, K. H. (2018). Simple Preparation of Cuprous Oxide Nanoparticles for Catalysis of Azide–alkyne Cycloaddition. *Journal of Chemical Research*, 42(3), 166–169. <https://doi.org/10.3184/174751918x15221562069666>
- Subash, B., Krishnakumar, B., Swaminathan, M., & Shanthi, M. (2013). Highly Efficient, Solar Active, and Reusable Photocatalyst: Zr-Loaded Ag–ZnO for Reactive Red 120 Dye Degradation with Synergistic Effect and Dye-Sensitized Mechanism. *Langmuir*, 29(3), 939–949. <https://doi.org/10.1021/la303842c>
- Jay Chithra, M., Sathya, M., & Pushpanathan, K. (2015). Effect of pH on Crystal Size and Photoluminescence Property of ZnO Nanoparticles Prepared by Chemical Precipitation Method. *Acta Metallurgica Sinica (English Letters)*, 28(3), 394–404. <https://doi.org/10.1007/s40195-015-0218-8>
- Oprea, O., Andronescu, E., Vasile, B., Voicu, G., & Covaliu, C. (2011). Synthesis and Characterization Of ZnO Nanopowder By Non-Basic Route. *Digest Journal of Nanomaterials and Biostructures*, 6, 1393–1401. https://chalcogen.ro/1393_Oprea.pdf
- Butte, S. M., & Waghuley, S. A. (2020). Optical properties of Cu₂O and CuO. *AIP Conference proceedings*. <https://doi.org/10.1063/5.0001644>
- Zhang, X., Song, J., Jiao, J., & Mei, X. (2010). Preparation and photocatalytic activity of cuprous oxides. *Solid State Sciences*, 12(7), 1215–1219. <https://doi.org/10.1016/j.solidstatesciences.2010.03.009>
- Joshi, S., Ippolito, S. J., & Sunkara, M. V. (2016). Convenient architectures of Cu₂O/SnO₂ type II p–n heterojunctions and their application in visible light catalytic degradation of rhodamine B. *RSC Advances*, 6(49), 43672–43684. <https://doi.org/10.1039/c6ra07150c>
- Winkler, N., Edinger, S., Kaur, J., Wibowo, R. A., Kautek, W., & Dimopoulos, T. (2018). Solution-processed all-oxide solar cell based

on electrodeposited Cu_2O and ZnMgO by spray pyrolysis. *Journal of Materials Science*, 53(17), 12231–12243. <https://doi.org/10.1007/s10853-018-2482-2>

Cui, J., & Gibson, U. J. (2010). A Simple Two-Step Electrodeposition of $\text{Cu}_2\text{O}/\text{ZnO}$ Nanopillar Solar Cells. *The Journal of Physical Chemistry C*, 114(14), 6408–6412. <https://doi.org/10.1021/jp1004314>